$K_5LaLi_2F_{10}:Er^{3+}$ crystals. Growth, structure and optical properties

1999 J. Phys.: Condens. Matter 11 5245

(http://iopscience.iop.org/0953-8984/11/27/302)

J. Phys.: Condens. Matter **11** (1999) 5245–5256. Printed in the UK PII: S0953-8984(99)01916-5

$K_5LaLi_2F_{10}:Er^{3+}$ crystals. Growth, structure and optical properties

G Dominiak-Dzik, S Gołab, M Bałuka, A Pietraszko and K Hermanowicz

Institute of Low Temperature and Structure Research, Polish Academy of Sciences, 2 Okólna Street, 50-950 Wrocław, Poland

Received 17 February 1999, in final form 12 April 1999

Abstract. Single crystals of $K_5LaLi_2F_{10}:Er^{3+}$ and $K_5LaLi_2F_{10}$ were synthesized and the structural determination was made by x-ray diffraction analysis. The structure is orthorhombic with space group *Pnma*. The unit cell parameters are: $a = 20.775$, $b = 7.822$ and $c = 6.963$ Å. The infrared transmission and Raman scattering spectra of oriented single crystals were measured and discussed in terms of factor group analysis and x-ray structure. A vibrational assignment is proposed. Preliminary optical properties of Er^{3+} ions in $K_5LaLi_2F_{10}$ crystals have been investigated using absorption, luminescence and lifetime measurements in the 5–300 K temperature range. The low temperature absorption and luminescence spectra of Er^{3+} have allowed us to identify the Stark levels of low-lying multiplets. The luminescence observed at 5 K has been attributed to the $^4S_{3/2} \rightarrow {}^4I_{15/2}$ (18 300 cm^{-1}), $^4F_{9/2} \rightarrow {}^4I_{15/2}$ (15 000 cm^{-1}), $^4S_{3/2} \rightarrow {}^4I_{13/2}$ (11800 cm^{-1}) and $^4I_{11/2} \rightarrow {}^4I_{15/2}$ (10000 cm^{-1}) transitions. The lifetimes of selected excited states were measured at 5 and 300 K temperature. The obtained data gave the first insight into the luminescent properties of Er^{3+} ions in the fluorine surroundings in $K_5LaLi_2F_{10}$ crystals.

1. Introduction

During the last few years there has been great interest in the study of rare-earth-doped fluoride. The fluoride systems provide a transparency from the ultraviolet to the infrared region and relatively low phonon energies of order 350–500 cm^{-1}. Such low lattice frequencies strongly suppress the nonradiative (multiphonon) relaxation for the most of the lanthanide excited states improving the light emission.

This paper deals with crystal growth, crystallographic structure, vibrations of the lattice and preliminary spectroscopic investigation of Er^{3+} doped $K_5LaLi_2F_{10}$ crystals. As luminescent systems, $K_5LnLi_2F_{10}$ (Ln = rare earth ions) crystals are uncommon in that the LnF_8 polyhedra in their crystal structure do not share fluorine atoms. Consequently, rare earth ions are well isolated and spaced apart. The activator–activator interaction is expected to be weak in these systems. Indeed, the $K_5NdLi_2F_{10}$ crystal is found to be an efficient luminescent material [1, 2], joining the group of so called stoichiometric luminescent compounds. According to the definition giving in [3], the term 'stoichiometric luminescent compounds' or 'self-activated-compounds' is being used to denote a compound in which the active ions like lanthanide ions enter not as a dopant but at the maximum concentration allowed by the chemical formula. In spite of high active-ion concentration luminescence quenching is strongly reduced in these systems. Among the stoichiometric luminescent compounds the oxide-coordinated Nd laser materials such as $MeNdP_4O_{12}$ (Me = Li, Na, K), NdP_5O_{14}, $NdAl_3(BO_3)_4$, $NdNa_5(WO_4)_4$ and $K_5Nd(MoO_4)_4$ are the best known [3–6].

0953-8984/99/275245+12$30.00

To our knowledge, erbium-doped $K_5LaLi_2F_{10}$ crystals have not been synthesized and studied before. Stability and conditions of the crystal growth of $K_5LaLi_2F_{10}$–$K_5ErLi_2F_{10}$ solid solutions are being examined now in our laboratory. In this paper basic properties of $K_5La_{0.95}Er_{0.05}Li_2F_{10}$, composed in the form of a large single crystal, are reported.

2. Experimental details

2.1. Crystal growth

The nominally anhydrous fluorides LiF, KF, LaF_3 and ErF_3, of 4N purity, were used as the starting materials. All the chemicals were dried under vacuum at about 200 °C to remove traces of water. The stoichiometric mixture of fluorides was heated at about 830 °C for 2 hours to prepare solid-state material. After cooling down, the obtained product was ground to powder and stored in a graphite crucible. The above procedure was carried out in an argon-filled glove box.

Single crystals of $K_5LaLi_2F_{10}$ and $K_5La_{0.95}Er_{0.05}Li_2F_{10}$ were obtained by the Bridgman method. The crystals were grown in pure argon atmosphere in graphite crucibles. The melting point of the mixture was 540 °C. The temperature gradient of the furnace was 120 °C cm^{-1} and the pulling rate was 1 mm h^{-1}.

In this way we obtained crystals of 4 mm diameter and a length of 20–30 mm. The x-ray structure determination proved the existence of one phase only. To eye the crystals were transparent but the absorption measurement showed that scattering centres are present.

2.2. Measurement techniques

The x-ray study was performed using a full automatic diffractometer with CCD detector. The infrared measurements were performed with an FTS 575C Bio-Rad spectrometer at room temperature. The Raman spectra were recorded with a DFS-24 LOMO monochromator by a cooled GaAs photomultiplier in a counting detection system. The spectral resolution was 2 cm^{-1}. Argon (ILA 120) and krypton (ILK 120) lasers were used as excitation sources. The measurements with polarized light were carried out for crystals oriented by the x-ray method.

Absorption spectra were measured with a Varian model 2300 spectrophotometer at 300 and 5 K. The spectral resolution was 0.2 nm in UV–VIS and 0.8 nm in the IR region. Low temperature (5 K) luminescence was excited by the 514 nm line of an argon ion laser. The spectra were analysed with a Zeiss model GDM 1000 grating monochromator (with a bandwidth of 2 cm^{-1}) and detected by a cooled photomultiplier. An SRS 250 boxcar integrator averaged a resulting signal. In luminescence decay time measurements a nitrogen-laser-pumped tunable dye laser was used as excitation source. For low temperature measurements the sample was placed in an Oxford model CF 1204 continuous flow helium cryostat equipped with a temperature controller.

3. $K_5LaLi_2F_{10}$:Er^{3+} crystal structure

The x-ray structure determination performed on small $K_5La_{1-x}Er_xLi_2F_{10}$ single crystals indicated that the structure is orthorhombic with the space group D_{2h}^{16}—$Pnma$, full symbol $P\frac{2_1}{n}\frac{2_1}{m}\frac{2_1}{a}$. The unit cell parameters are $a = 20.775$, $b = 7.822$ and $c = 6.963$ Å. It was found that there are 3.75 La and 0.25 Er atoms, eight Li atoms, 20 K and 40 F atoms per unit cell. Eight fluorine F atoms coordinate each La atom. The point symmetry for the La^{3+} sites was determined to be C_s. Erbium ions enter as a dopant into the $K_5LaLi_2F_{10}$ lattice replacing

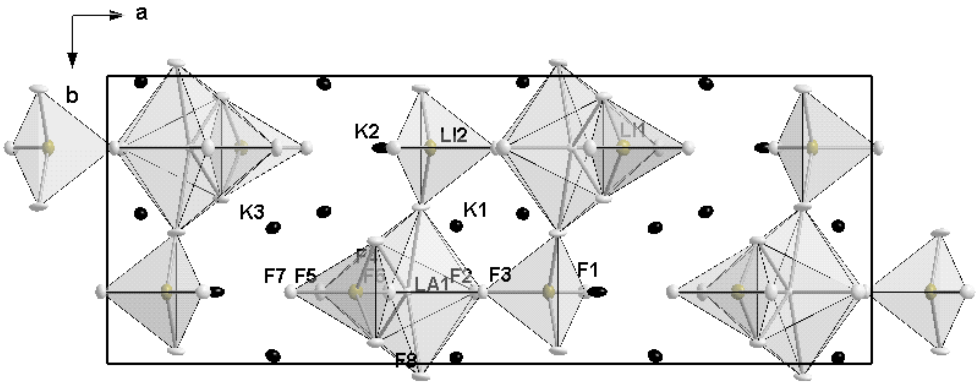

Figure 1. Crystal structure of $K_5La_{0.95}Er_{0.05}Li_2F_{10}$ in the *ab* projection.

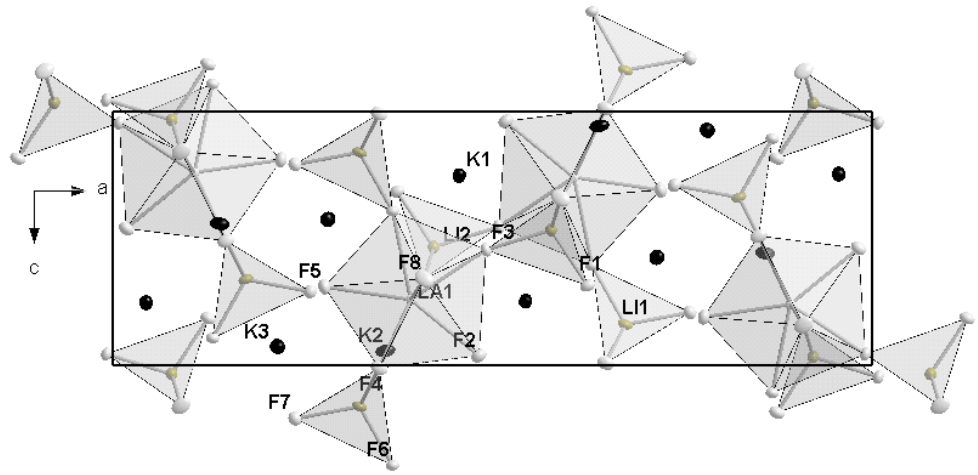

Figure 2. Projection of the crystal structure along the *b* axis for the $K_5La_{0.95}Er_{0.05}Li_2F_{10}$ crystal.

lanthanum ions in their sites. Lithium atoms occupy the C_s symmetry sites too, whereas the symmetry of the potassium and fluorine sites is both C_s and C_1. The crystal structure projection on *ab* and *ac* planes is presented in figures 1 and 2. The basic structural features of the $K_5LaLi_2F_{10}$ crystal are sheets perpendicular to the *a* axis, formed by isolated LaF_8 dodecahedra and LiF_4 tetrahedra. The sheets are clasped by the K^+ ions. Each LaF_8 dodecahedron is surrounded by 12 others and is connected by Li^+ ions along the *b* and *c* axes. The Wyckoff positions, the atomic coordinates, the equivalent isotropic displacement parameters U_{eq} and occupancy factors are given in table 1. The bond lengths for $K_5La(Er)Li_2F_{10}$ are gathered in table 2.

The $K_5LaLi_2F_{10}$ crystal structure is closely related to the structure of the $K_5NdLi_2F_{10}$ crystal [1], the first reported fluoride compound in which the Nd polyhedra are isolated from each other. This means that the polyhedra do not share F atoms and the shortest Nd–Nd distance is 6.72 Å. An isolation of the active ions from their surroundings provides reduction of nonradiative deactivation and, in consequence, relatively little concentration quenching.

Table 1. Atomic coordinates and equivalent isotropic displacement parameters U_{eq} ($A^{-2} \times 10^{-3}$) for $K_5La_{0.95}Er_{0.05}Li_2F_{10}$. $U_{(eq)}$ is defined as one third of the trace of the orthogonalized U_{ij} tensor. Space group $Pnma$.

Atom	Wyckoff position	Atomic coordinates			U_{eq}	Occupancy factor
		x	y	z		
La(1)	4c	0.1076(1)	0.2500	0.2406(1)	7(1)	0.95
Er(1)	4c	0.1076(1)	0.2500	0.2406(1)	7(1)	0.05
K(1)	8d	0.0437(1)	0.0215(1)	0.7528(1)	15(1)	1
K(2)	4c	0.8592(1)	0.2500	0.5577(2)	18(1)	1
K(3)	8d	0.2168(1)	0.9723(1)	0.9250(1)	17(1)	1
F(1)	4c	0.8746(2)	0.2500	0.1855(5)	16(1)	1
F(2)	4c	0.0178(2)	0.2500	0.4611(5)	18(1)	1
F(3)	4c	0.0085(2)	0.2500	0.0450(4)	14(1)	1
F(4)	8d	0.1491(1)	0.0734(4)	0.5095(3)	15(1)	1
F(5)	4c	0.2214(2)	0.2500	0.1910(5)	19(1)	1
F(6)	4c	0.1315(2)	0.2500	0.8927(4)	16(1)	1
F(7)	4c	0.7602(2)	0.2500	0.7909(5)	16(1)	1
F(8)	8d	0.0899(1)	0.9548(3)	0.1591(4)	19(1)	1
Li(1)	4c	0.6750(5)	0.2500	0.8386(13)	15(2)	1
Li(2)	4c	0.9226(5)	0.2500	0.9665(14)	15(2)	1

Standard deviations are given in parentheses.

4. Vibrational analysis of the lattice

The structural data form the basis for the theoretical analysis of vibrational features. The 72 atoms of the unit cell give rise to 216 fundamental vibrations expected in the $k = 0$ approximation. The irreducible representations and activities calculated for the unit-cell vibrations near the Brillouin zone are presented in table 3. The unit cell modes were resolved into parts corresponding to acoustic (T), external (L—libratory and T′—translatory lattice vibrations) and internal (i) modes. The last column gives information about mode activity in the infrared and Raman spectra presented in figure 3. The band assignment, vibrational wavenumbers and relative intensities of the observed bands are given in table 4. The description of the spectra was based upon previous studies performed for a simple fluoride elpasolite Cs_2MLnF_6 where $M = K^+$, Na^+ ions and Ln means lanthanide ions [7–12].

The vibrational spectra of the studied compound are very complex as compared to the simple fluoride elpasolites [12]. These cubic compounds contain octahedrally coordinated LnF_6^{-3} polyhedrons, which have simple vibrational characteristics. For an octahedral molecule six normal modes of vibrations are distributed among Raman active stretching $\nu_1(A_{1g})$, $\nu_2(E_g)$ and bending $\nu_5(F_{2g})$ modes. The stretching $\nu_3(F_{1u})$ and bending $\nu_4(F_{1u})$ are observed in the IR spectra whereas the $\nu_6(F_{2u})$ mode is IR and Raman inactive and usually can be obtained from the vibronic transitions of the electronic absorption and emission spectra [13, 14]. The energetic position of these modes is well known [6–12]. The normal vibrations of the lanthanide Cs_2MLnF_6 elpasolites were assigned to the bands in the regions ν_1: 450–500, ν_2: 340–405, ν_3: 370–425, ν_4: 150–180, ν_5: 160–210 and ν_6: 90–130 cm^{-1}. This data set could not be immediately applied to the analysis of the vibrational spectra measured for the $K_5LaLi_2F_{10}$ crystals. Two basic structural units are present in its unit cell: LaF_8 dodecahedra and LiF_4 tetrahedra. The former polyhedron could be an undistorted cube (O_h symmetry), square antiprism (D_{4d} symmetry) or dodecahedron (D_{2d} symmetry). The antiprism is obtained by starting with a cube and rotating the top in its own plane by 45° with respect to the base.

Table 2. Bond lengths (Å) for $K_5La_{0.95}Er_{0.05}Li_2F_{10}$.

Fluoride around La (Er) atom (dodecahedron)		Tetrahedron around La (Er) atom	
La(1)–F(5b)	2.391(4)	La(1)–Li(1)	3.249(9)
La(1)–F(8a)	2.405(3)	La(1)–K(1)	3.7928(12)
La(1)–F(8b)	2.405(3)	La(1)–K(1)	3.7928(12)
La(1)–F(2b)	2.415(3)	La(1)–K(3)	3.8336(10)
La(1)–F(3b)	2.468(3)		
La(1)–F(6a)	2.473(3)		
La(1)–F(4b)	2.482(3)		
La(1)–F(4d)	2.482(3)		
Coordination sphere of K(1)		Coordination sphere of K(2)	
K(1)–F(2)	2.758(3)	K(2)–F(1)	2.611(4)
K(1)–F(2)	2.892(3)	K(2)–F(4)	2.578(3)
K(1)–F(3)	2.805(3)	K(2)–F(4)	2.578(3)
K(1)–F(3)	2.769(2)	K(2)–F(7)	2.620(4)
K(1)–F(4)	2.798(3)	K(2)–F(8)	2.752(3)
K(1)–F(6)	2.733(3)	K(2)–F(8)	2.752(3)
K(1)–F(8)	2.849(3)	K(2)–Li(2)	3.136(10)
K(1)–Li(2)	2.970(7)	K(2)–F(2)	3.364(4)
K(1)–F(1)	2.753(3)	K(2)–F(5)	3.344(4)
K(1)–Li(1)	3.324(9)		
K(1)–Li(2)	3.426(9)		
Coordination sphere of K(3)		Tetrahedron around Li(1)	
K(3)–F(1)	2.686(3)	Li(1)–F(4)	1.821(6)
K(3)–F(4)	2.870(3)	Li(1)–F(4)	1.821(6)
K(3)–F(5)	2.706(3)	Li(1)–F(6)	1.847(10)
K(3)–F(5)	2.857(3)	Li(1)–F(7)	1.800(11)
K(3)–F(6)	2.813(2)		
K(3)–F(7)	2.677(3)	Tetrahedron around Li(2)	
K(3)–F(7)	2.792(2)		
K(3)–F(8)	3.102(3)	Li(2)–F(1)	1.822(10)
K(3)–Li(1)	2.973(6)	Li(2)–F(8)	1.844(5)
K(3)–Li(1)	3.284(9)	Li(2)–F(8)	1.844(5)
K(3)–F(4)	3.312(3)	Li(2)–F(3)	1.867(11)
K(3)–Li(2)	3.460(9)		

Therefore, the eight ligands should be equivalent for the cube and the antiprism. In the dodecahedral structure the eight ligands are divided into two non-equivalent sets of four in each set. The vibrations of the LaF_8 system are described by 21 fundamental modes, expressed for the respective structure in the following form:

$$T_{(O_h)} = A_{1g}(R) + A_{2u}(ia) + E_g(R) + E_u(ia) + 2F_{1u}(IR) + 2F_{2g}(R) + F_{2u}(ia)$$
$$T_{(D_{4d})} = 2A_1(R) + B_1(ia) + 2B_2(IR) + 3E_1(IR) + 3E_2(R) + 2E_3(R)$$
$$T_{(D_{2d})} = 4A_1(R) + A_2(ia) + 2B_1(R) + 4B_2(R, IR) + 5E(R, IR).$$

This means that the IR and Raman spectra could be the probe for the structure of the LnF_8 polyhedron present in the crystal. For the cubic symmetry one stretching $\nu(F_{1u})$ and one deformation $\delta(F_{1u})$ band should be expected as active in the infrared spectra. In the Raman spectra we should observe two stretching $\nu(A_{1g})$ and $\nu(E_g)$ and two bending $\delta(F_{2g})$ modes. For the D_{2d} symmetry four stretching $(2B_2 + 2E)$ frequencies ν(La–F) and five bending $(2B_2 + 3E)$

Table 3. Vibrational analysis of $K_5LaLi_2F_{10}$ crystal.

D_{2h}^{16} space group	Vibrational degrees of freedom n_i(N)	Acoustic modes n_i(T)	Translational lattice modes n_i(T′)	Librational lattice modes n_i(L)	Internal modes of the four LaF_8 units n_i(i)	Activity	
						IR	Raman
A_g	32	0	17	2	13	–	xx, yy, zz
B_{1g}	22	0	13	1	8	–	xy
B_{2g}	32	0	17	2	13	–	xz
B_{3g}	22	0	13	1	8	–	yz
Au	22	0	13	1	8	–	–
B_{1u}	32	1	16	2	13	z	–
B_{2u}	22	1	12	1	8	y	–
B_{3u}	32	1	16	2	13	x	–
Overall	216	3	117	12	84		

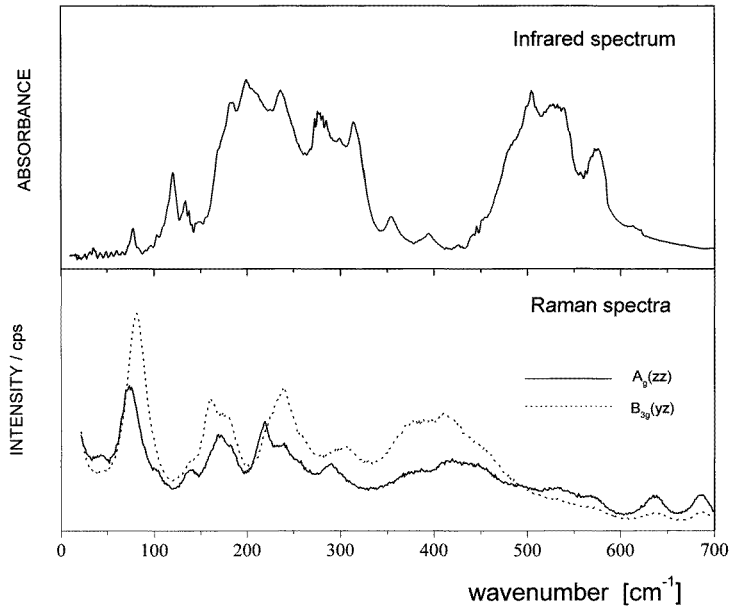

Figure 3. The infrared (upper picture) and Raman spectra of a $K_5LaLi_2F_{10}$:Er single crystal recorded at room temperature.

ones should be observed in the infrared region whereas in the Raman spectra six stretching ($2A_1 + 2B_2 + 2E$) and nine bending ($2A_1 + 2B_1 + 2B_2 + 3E$) modes should be active. Since the lanthanide ions occupy the C_s symmetry sites all these modes became active both in the infrared and Raman spectra. On the basis of the above consideration certain conclusions on the structure of the LnF_8 unit can be drawn that will be useful for the band assignment. In the range 400–550 cm^{-1} four distinct lines are observed in Raman spectra and six bands in the infrared spectrum. Their contours have multiplet character because several weak components and shoulders are present on the slope of main bands due to the factor group splitting. In the range 150–350 cm^{-1} where the bending δ(F–La–F) vibrations are expected complex patterns are observed both in the IR and Raman spectra. In the Raman contour six-seven components

Table 4. Wavenumbers and tentative assignment of the bands observed in the IR and Raman spectra of the $K_5LaLi_2F_{10}$ crystal.

Wavenumber ν [cm^{-1}]			
	Raman spectrum		
Infrared spectrum	$A_g(zz)$	$B_{3g}(yz)$	Band assignment
—	684 w	686 vw	Probably ν(Li–F) stretching vibrations
620 w	635 w	635 vw	
614 w	—	—	
573 s	568 w	569 vw	
536 vs	533 w	532 vw	
527 vs	—	—	
505 vs	—	—	ν(La–F) stretching vibrations
484 sh	493 w	—	
440 w	446 m	448 sh	
426 vw	417 m	407 s	
394 w	386 m	374 s	ν(La–F–Li)
354 m	—	—	
315 m	—	—	
299 m	289 m	303 m	T′(Li) or δ(F–Li–F) bending vibrations
285 s	—	—	
278 m	254 sh	258 sh	δ(F–La–F) bending vibrations
236 s	240 m	237 s	
208 sh	219 s	—	and
198 vs	—	—	
184 s	181 m	176 s	T′(K) lattice vibrations
170 sh	170 s	160 s	
134 m	139 m	139 sh	
121 s	102 sh	—	L(LaF_8) and T′(La) lattice vibrations
78 m	74 vs	83 vs	
35 vw	42 m	—	

s—strong, vs—very strong, m—medium, w—weak, vw—very weak, sh—shoulder.

can be subdivided and nine/ten bands in the IR spectrum. This means that the vibrational spectra are consistent with the eightfold coordination of the LnF_8 polyhedron and its structure is close to the dodecahedron. The vibrations of the LiF_4 tetrahedron are also reflected in the vibrational spectra. Their wavenumbers lie in higher energy regions, i.e. at 560–690 cm^{-1} for stretching modes and 300–400 cm^{-1} for bending ones. Several other bands observed in the far infrared regions correspond to the translatory lattice modes: T′(K) (170–190 cm^{-1}) and T′(Li) (270–320 cm^{-1}). The strongest Raman lines in the 74–105 cm^{-1} range were assigned to the libratory L(LaF_8) mode with A_g symmetry (at 74 and 102 cm^{-1}) and the B_{3g} one (at 83 cm^{-1}). It should be pointed out that some of the Raman bands are strongly polarized. These are lines at about 680, 635, 303, 290, 220 and 140 cm^{-1}.

5. Optical properties

5.1. Absorption data

The room temperature absorption spectrum of the $K_5LaLi_2F_{10}$:Er^{3+} crystal is shown in figure 4. It consists of ten bands associated with transitions from the $^4I_{15/2}$ ground state to the excited states, marked on the picture. They are situated in the near infrared and the visible spectral

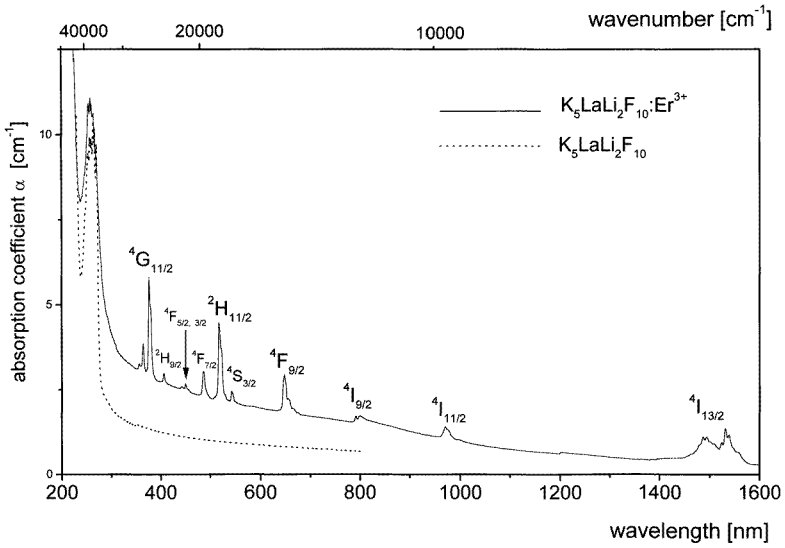

Figure 4. Absorption spectrum of Er^{3+} ions in $K_5LaLi_2F_{10}$ crystal (solid line) and absorption spectrum of $K_5LaLi_2F_{10}$ matrix (dotted line). $T = 300$ K.

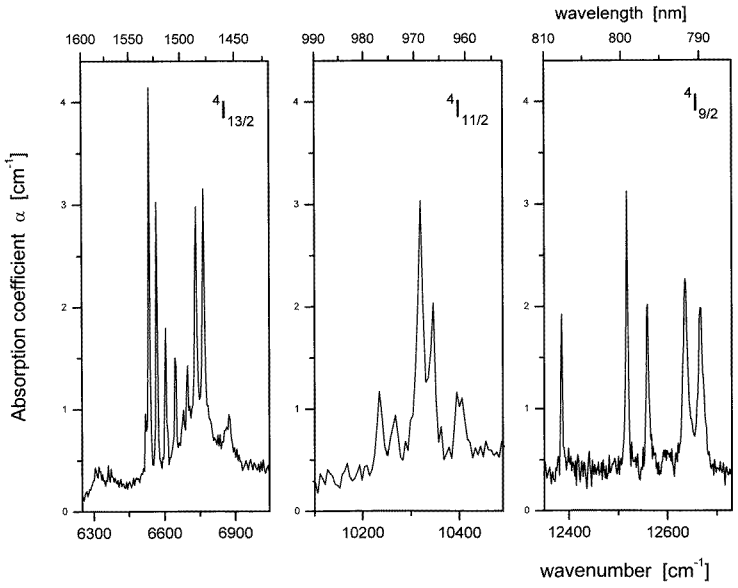

Figure 5. Absorption spectra of the $^4I_{15/2} \rightarrow {}^4I_{13/2}$, $^4I_{11/2}$ and $^4I_{9/2}$ transitions of Er^{3+} ions in the $K_5LaLi_2F_{10}$ crystal at 5 K temperature.

region. In addition, the absorption spectrum of the $K_5LaLi_2F_{10}$ crystal recorded in the 800–228 nm spectral range at 300 K is shown in this figure. In the ultraviolet spectral region, the absorption spectrum of $K_5LaLi_2F_{10}$ as well as the absorption spectrum of $K_5LaLi_2F_{10}$:Er^{3+} has a band situated at about 260 nm. Its origin is not clear. The intensity of this band and

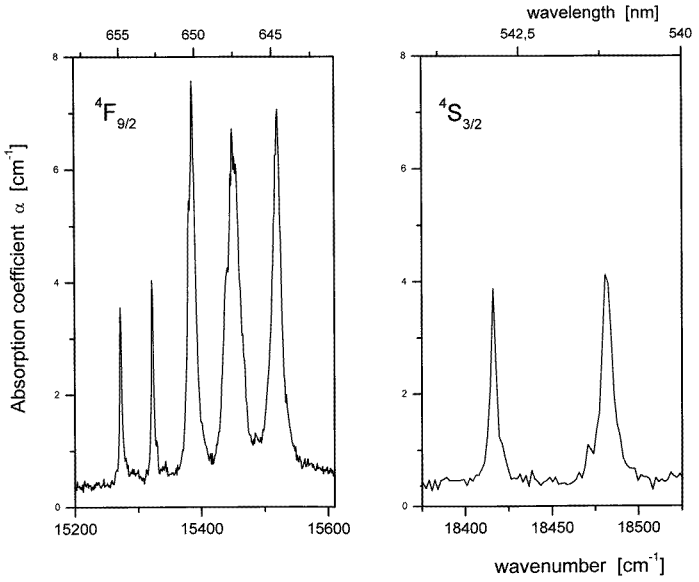

Figure 6. Low temperature absorption from the $^4I_{15/2}$ ground state of Er^{3+} to the $^4F_{9/2}$ and the $^4S_{3/2}$ excited states in the $K_5LaLi_2F_{10}$ matrix.

Table 5. Energies of crystal field levels and overall splitting of selected multiplets of Er^{3+} ion in $K_5LaLi_2F_{10}$ crystal.

Multiplet	Energy [cm^{-1}]	ΔE [cm^{-1}]	Component number theor./exp.
$^4I_{15/2}$	0, 28, 63, 94, 135, 224, 281, 494	494	8/8
$^4I_{13/2}$	6536, 6566, 6605, 6647, 6698, 6733, 6765	229	7/7
$^4I_{11/2}$	10 235, 10 267, 10 320, 10 345, 10 395, 10 405	170	6/6
$^4I_{9/2}$	12 385, 12 517, 12 559, 12 636, 12 667	282	5/5
$^4F_{9/2}$	15 272, 15 322, 15 386, 15 449, 15 521	250	5/5
$^4S_{3/2}$	18 416, 18 481	65	2/2

its location indicate that probably this absorption is due to point defects of the lattice as it is observed in other crystals [15]. It is worth noting that the measured value of the absorption coefficient is too low to give any information about the ultraviolet absorption edge of the matrix. Thus, the real edge of the lattice absorption is situated at about 230 nm or less.

In figures 5 and 6 we present absorption spectra measured at 5 K. They were used to determine the energy and the Stark components of Er^{3+} ion levels in the $K_5LaLi_2F_{10}$ crystal. The crystal-field levels of the $^4I_{15/2}$ ground state were derived from the $^4S_{3/2} \rightarrow {}^4I_{15/2}$ and the $^4I_{11/2} \rightarrow {}^4I_{15/2}$ luminescence spectra recorded also at 5 K temperature. The assignment of Er^{3+} ion levels in $K_5LaLi_2F_{10}$, the number and the energy of the Stark components are gathered in table 5. Taking into account a high multiplicity of Er^{3+} ions ($4f^{11}$ electronic structure) and very low symmetry of the Er sites we can expect that the energy levels will split into $(J + \frac{1}{2})$ Stark components. From table 5 it can be seen that the experimentally identified number of the Stark components is in accordance with theory.

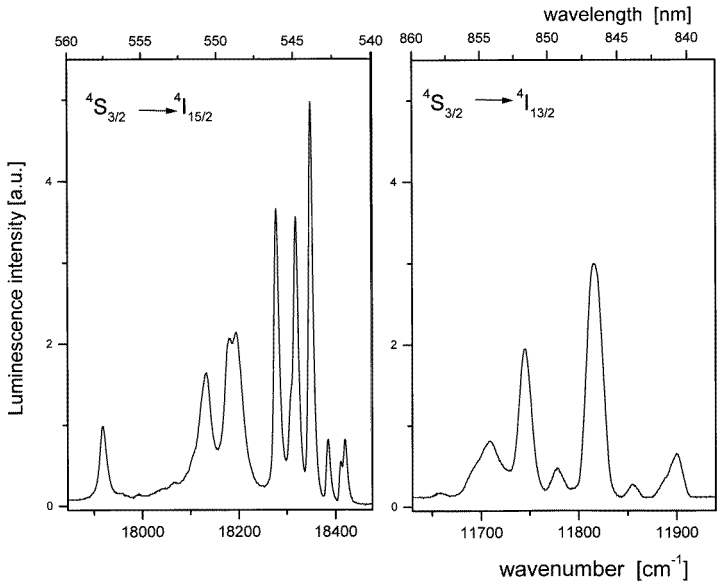

Figure 7. Luminescence spectra of Er^{3+} in the $K_5LaLi_2F_{10}$ crystal associated with the $^4S_{3/2} \rightarrow {}^4I_{15/2}$ and the $^4S_{3/2} \rightarrow {}^4I_{13/2}$ transitions. $T = 5$ K.

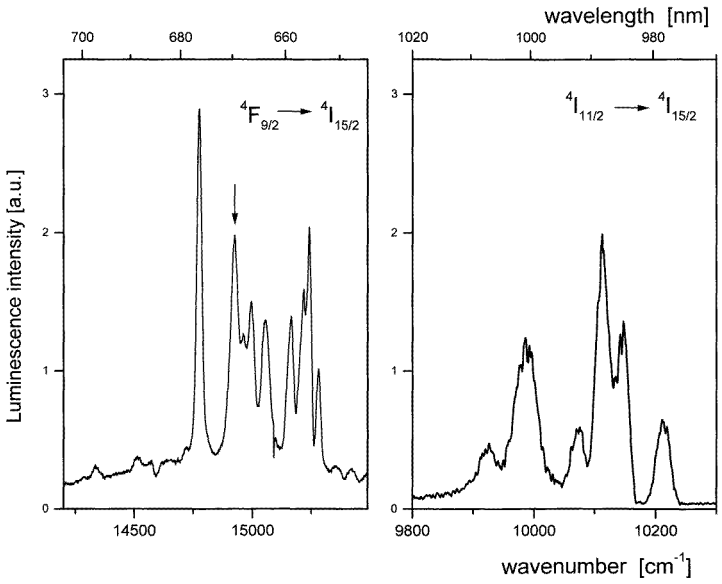

Figure 8. Emission from the $^4F_{9/2}$ and the $^4I_{11/2}$ states to the $^4I_{15/2}$ ground state of Er^{3+} in the $K_5LaLi_2F_{10}$ crystal measured at 5 K. (Explanation of the arrow is given in the text.)

5.2. Fluorescence data—emission spectra and lifetimes

Er^{3+} ion luminescence was studied at 300 and 5 K. The available argon laser was suitable for exciting the $^2H_{11/2}$ multiplet of the Er^{3+} ion in the 19 000 cm^{-1} region. Low temperature emission is presented in figures 7 and 8. Figure 7 shows emission from the $^4S_{3/2}$ excited

state to the $^4I_{15/2}$ ground state and to the $^4I_{13/2}$ excited multiplet. Emission lines observed at 15 000 cm^{-1} were assigned to the $^4F_{9/2} \rightarrow {}^4I_{15/2}$ transition and the luminescence spectrum associated with the $^4I_{11/2} \rightarrow {}^4I_{15/2}$ one appears near 1.0 μm. They are presented in figure 8. We were not able to measure emission from the $^4I_{13/2}$ state that occurs at about 1.6 μm because of experimental limitations. This limitation did not allow us to verify the existence of the interstate fluorescence $^4I_{11/2} \rightarrow {}^4I_{13/2}$ appearing in the 2.7–2.9 μm spectral range.

All luminescence transitions from excited states to the $^4I_{15/2}$ level give insight into the Stark level structure of the ground level. For the $^4S_{3/2} \rightarrow {}^4I_{15/2}$ we observed transitions from the $^4S_{3/2}$ excited state to all Stark components of the $^4I_{15/2}$ ground state. In the case of the $^4I_{11/2} \rightarrow {}^4I_{13/2}$ transition we observed six instead of eight peaks in the spectrum. A detailed analysis indicates that the transitions to two components of the ground state are not present. The spectrum of the $^4F_{9/2} \rightarrow {}^4I_{15/2}$ transition consists of eight peaks, but only seven of them are consistent with the ground state splitting derived from transitions originating in the $^4S_{3/2}$ and the $^4I_{11/2}$. The origin of the additional peak at 14 923 cm^{-1} (marked by the arrow in figure 8) is not clear, yet.

The lifetime measurements of the emitting levels have been made at 5 and 300 K temperature under excitation with 815 nm for the $^4I_{11/2}$ level and with 532 nm for the $^4S_{3/2}$ multiplet. The $^4I_{9/2}$ state was excited directly ($\lambda_{exc} = 815$ nm) and its lifetime was estimated to be 450 μs both at 300 and 5 K temperature. Results of the lifetime measurements are gathered in table 6. It can be seen that unlike the $^4S_{3/2}$ lifetime the temperature influences the lifetime for the $^4I_{11/2}$ level. Taking into account the highest phonon energy ($\nu_{ph} = 680$ cm^{-1}) and the energy gap between the $^4I_{11/2}$ level and the lower lying $^4I_{13/2}$ state of 3700 cm^{-1}, we suppose that the multiphonon processes are active. Contribution of ion–phonon and ion–ion interaction to the relaxation of excited states of Er^{3+} in $K_5LaLi_2F_{10}$ is to be determined. To do this we are preparing crystals containing lower Er^{3+} concentration.

Table 6. Lifetimes τ of some relevant excited states in $K_5LaLi_2F_{10}$:Er^{3+} crystal.

	Lifetime τ[ms]	
Multiplet	5 K	300 K
$^4S_{3/2}$	0.459	0.442
$^4I_{11/2}$	3.75	2.70
$^4I_{9/2}$	0.450	0.450

6. Conclusion

We have grown undoped and erbium doped $K_5LaLi_2F_{10}$ single crystals. A full crystal structure and vibrational analysis has been made. The vibrational analysis gave information in relation to the matrix phonons showing that the most energetic vibrations are associated with the Li–F stretching vibrations ($\nu_{ph} = 680$ cm^{-1}).

The present optical studies (absorption, emission and lifetime) yield only a preliminary picture of the spectroscopic properties of Er^{3+} ions in $K_5LaLi_2F_{10}$ crystals. They are the beginning for future fundamental studies of excited state relaxation and processes determining the luminescence efficiency in fully concentrated $K_5LnLi_2F_{10}$ systems.

References

[1] McCollum B C and Lempicki A 1978 *Mater. Res. Bull.* **13** 883
[2] Hong H Y-P and McCollum B C 1979 *Mater. Res. Bull.* **14** 137

[3] Danielmeyer H G 1975 Stoichiometric laser materials *Festkörperprobleme (Advances in Solid State Physics)* vol 15 (Braunschweig: Pergamon) p 253
[4] Hong H Y-P 1974 *Acta Crystallogr.* B **30** 486
[5] Weber H P, Damen T C and Danielmeyer H G 1973 *Appl. Phys. Lett.* **22** 534
[6] Kaminskii A A, Sarkisov S E, Bohm J, Reiche P, Schultze D and Uecker R 1977 *Phys. Status Solidi* a **43** 71
[7] Thompson L C, Kuo S C and Amberger H D 1990 *New Developments in f-Elements* (Görller-Walrand) p 187
[8] Amberger H D 1978 *Inorg. Nucl. Chem. Lett.* **14** 491
[9] Amberger H D 1980 *Z. Anorg. (Allg.) Chem.* **467** 231
[10] Becker R, Leutz A and Sawodny W 1976 *Z. Anorg. (Allg.) Chem.* **420** 210
[11] Selgert P, Lingner C and Lüthi B 1984 *Z. Phys.* B **55** 219
[12] Tanner P A and Shen Merg-Yan AP-17-93 *Research Report City Polytechnic of Hong Kong Department of Applied Science*
[13] Jeżowska-Trzebiatowska B, Ryba-Romanowski W, Mazurak Z and Hanuza J 1980 *Chem. Phys.* **50** 209
[14] Tanner P A 1988 *Mol. Phys.* **63** 365
[15] Kovalyova N S, Ivanov A O and Dubrovina E P 1981 *Kvant. Elektron.* **8** 2433